Role of ICAM-3 in the initial interaction of T lymphocytes and APCs

María C. Montoya[1], David Sancho[1], Grégory Bonello[2], Yves Collette[2], Claire Langlet[3], Hai Tao He[3], Pedro Aparicio[4], Andrés Alcover[5], Daniel Olive[2] and Francisco Sánchez-Madrid[1]

Antigen-independent adhesive interactions between T lymphocytes and antigen-presenting cells (APCs) are essential for scanning for specific antigens on the APC surface and for initiating the immune response. Here we show, through time-lapse imaging of live cells, that the intercellular adhesion molecule 3 (ICAM-3, also known as CD50) is clustered specifically at the region of the T lymphocyte surface that initiates contact with APCs. We describe the role of ICAM-3 in T cell–APC conjugate formation before antigen recognition, in early intracellular signaling and in cytoskeletal rearrangement. Our data indicate that ICAM-3 is important in the initial scanning of the APC surface by T cells and, therefore, in generating the immune response.

The immune response is initiated when T lymphocytes recognize antigen peptides bound to major histocompatibility complex (MHC) molecules on the surface of APCs. T lymphocytes can interact with many different APCs in an antigen-independent manner[1]. Thus, exploratory adhesive interactions of T lymphocytes and APCs are essential for the specific recognition of antigenic peptides and for initiating the immune response. Different receptor-ligand pairs are involved in T cell–APC recognition, including T cell receptor (TCR)-peptide-MHC, CD2–leukocyte function antigen 3 (LFA-3), CD28-CD80 and LFA-1–intercellular cell adhesion molecule 1 (ICAM-1)[1]. But the reduced size of CD2, TCR and CD28, the very low affinity of the TCR and the nonactivated state of LFA-1 in resting cells make these molecules unlikely candidates for initiating intercellular adhesion.

An efficient adaptive immune response requires that, on antigen-TCR engagement, T lymphocytes develop a complex organization of molecules in the T cell–APC interface called the immunological synapse[1]. Adhesion, costimulatory, cytoskeletal and signaling molecules are organized in supramolecular activation clusters (SMACs), which comprise a central SMAC that includes TCR, CD28, CD3, CD2, protein kinase C-θ (PKC-θ), Lck, Fyn and a peripheral SMAC in which LFA-1 and talin are localized[2–6]. Synapse formation is accompanied initially by strong induction of tyrosine phosphorylation, Ca^{2+} mobilization and changes in the metabolism of inositol phospholipids. The nuclear factor NFAT is dephosphorylated on calcium mobilization during T cell activation and translocates to the nucleus, where it is crucial for expression of the gene encoding interleukin 2 (IL-2)[1]. Signaling mediated by the TCR induces cytoskeletal rearrangements, such as actin polymerization at the T cell–APC interface and reorientation of the microtubule-organizing center (MTOC) towards the immunological synapse[7].

Early TCR signaling involves the phosphorylation of CD3 subunits by Lck, which allows binding and activation of the ZAP-70 kinase[8,9].

Activated ZAP-70 phosphorylates the transmembrane protein linker for activation of T cells (LAT)—an adapter molecule that acts as a scaffold to localize and assemble signaling molecules, including phospholipase C-γ1 (PLC-γ1), Grb2, Grap, Src homology domain 2 (SH2)-containing leukocyte protein 76 (SLP76), Vav, Cbl and Gads-Grf40-Grpl, which are essential for TCR-dependent signal transduction[10,11]. For efficient signal transduction, the molecules that are essential for T cell activation must be associated constitutively with lipid rafts or redistributed into rafts after TCR engagement[12].

The adhesion molecule ICAM-3 belongs to the immunoglobulin superfamily and is structurally homologous to ICAM-1 and ICAM-2[13,14]. Much evidence suggests that this molecule may be involved in the initial steps of immune cell interactions—for example, there is high constitutive expression of ICAM-3 in resting T lymphocytes[15], ICAM-3 possesses costimulatory activity in T lymphocytes[16–19], ICAM-3 is localized at cell-cell contacts during initial cell aggregation and ICAM-3 can induce LFA-1–ICAM-1 adhesion[17]. Several ICAM-3 ligands have been identified, including the β2 integrin LFA-1, which forms low-affinity interactions with ICAM-3 in comparison to its interactions with ICAM-1[13,14], and $\alpha_d\beta_2$[20]. Dendritic-cell–specific ICAM-3 grabbing nonintegrin (DC-SIGN), a C-lectin molecule expressed by dendritic cells (DCs), has been identified as a high-affinity ligand for ICAM-3, which also suggests that this adhesion molecule is involved in primary immune responses[21]. But direct evidence showing that ICAM-3 has a role in the initial adhesion between T lymphocytes and APCs has not been reported.

We have analyzed the dynamic localization of ICAM-3 during the initial steps of T cell–APC interaction in comparison with the localization of other adhesion molecules and components of the immunological synapse, namely P-selectin glycoprotein ligand 1 (PSGL-1), which is the ligand for E-, P- and L-selectin, and the adapter molecule LAT. Our data indicate that ICAM-3 is involved in the initial exploratory contact of T cells with APCs that occurs before antigen-specific recognition. We

[1]Servicio de Inmunología, Hospital de la Princesa, C/ Diego de León 62, Universidad Autónoma de Madrid, 28006 Madrid, Spain. [2]Institut de Cancerologie et d'Immunologie de Marseille, Université de la Mediterranée, Institut Paoli Calmettes, Inserm U119, 27 Boulevard Lei Roure, 13009 Marseille, France. [3]Centre d'Immunologie de Marseille Luminy, Inserm CNRS, Case 906, 13288 Marseille, France. [4]Facultad de Medicina, Universidad de Murcia, Espinardo, 30100 Murcia, Spain. [5]Unité de Biologie des Interactions Cellulaires, CNRS URA 1960, Institut Pasteur, 28 rue du Dr. Roux, 75724 Paris Cedex 15, France. Correspondence should be addressed to F. S.-M. (fsanchez@hlpr.insalud.es).
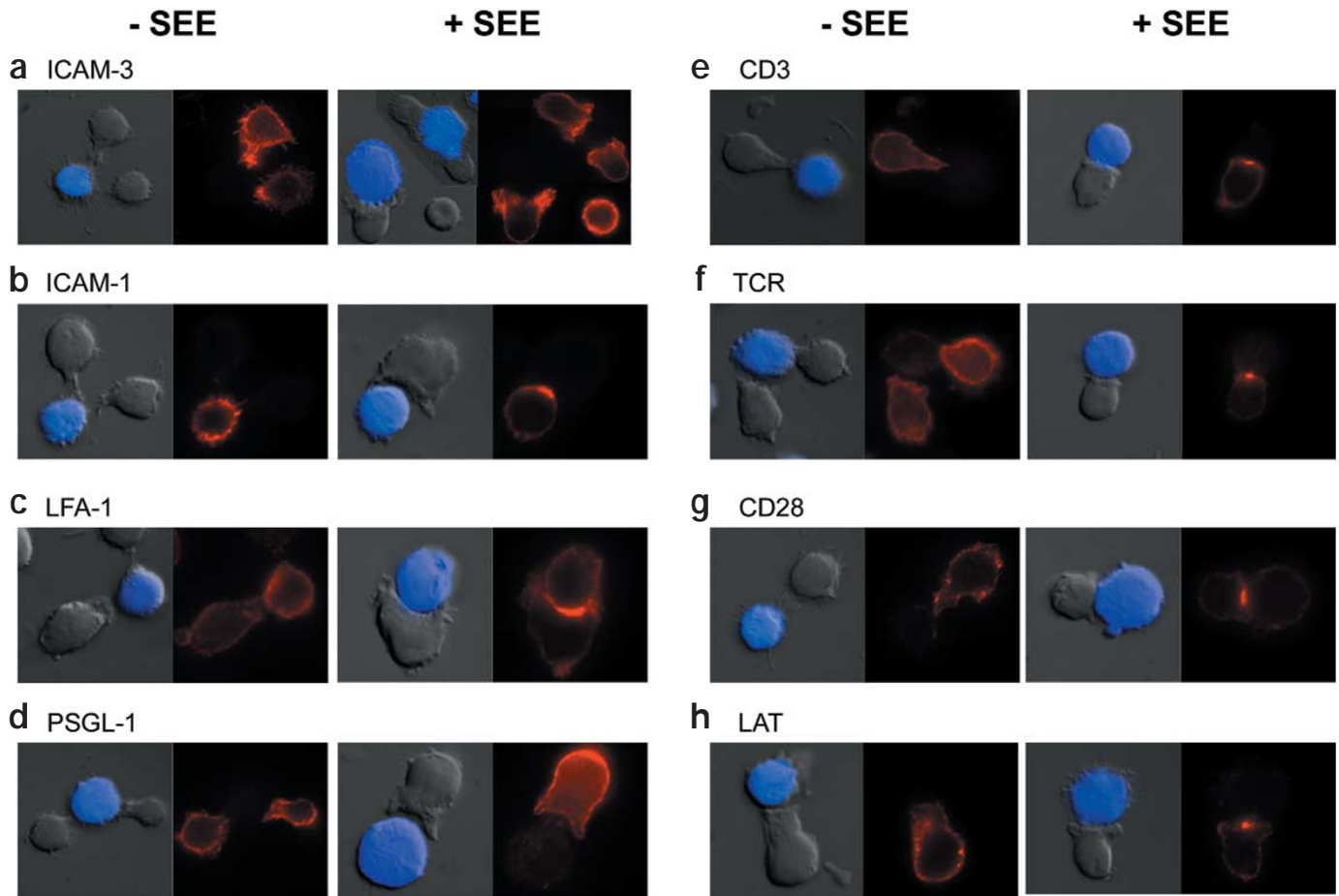
Figure 1. Localization of adhesion, costimulatory and signaling molecules in the T cell–APC conjugate. Raji cells were labeled with the blue fluorescent cytoplasmic probe CMAC, and then incubated (+SEE) or not (–SEE) with 5 g/ml of SEE. The Raji and Jurkat J77 cells were then mixed and adhered to PLL-coated coverslips for 10 min at 37 °C. (Right) Conjugates were fixed and stained (in red) for ICAM-3 (**a**), ICAM-1 (**b**), LFA-1 (**c**), PSGL-1 (**d**), CD3 (**e**), TCR (**f**), CD28 (**g**) or LAT (**h**). (Left) The corresponding DIC images were superimposed on blue staining of Raji cells.

found that ICAM-3 has a costimulatory effect in TCR-induced signaling events including phosphorylation of LAT, activation of NFAT and the cytoskeletal rearrangements that lead to MTOC translocation.

Results

ICAM-3 clusters at the T cell–APC contact region

To identify molecules involved in the initial exploration of APCs by T lymphocytes, we studied the localization of ICAM-3 and other adhesion and costimulatory molecules in T cell–APC conjugates. We examined interactions between $V_\beta 8$ TCR–expressing Jurkat cells and the human B cell line Raji. Jurkat cells can be stimulated by superantigen staphylococcal enterotoxin E (SEE)[22] and showed characteristics of naïve T cells, including very low expression of ICAM-1 and expression of LFA-1 in a low-affinity binding state (data not shown). These cells were not polarized and expressed high amounts of ICAM-3, which were distributed uniformly on the cell surface (**Fig. 1a**). In the absence of SEE signals, ICAM-3, but not the other adhesion or costimulatory receptors that we assayed, clustered to the T cell surface region that contacts the APC (**Fig. 1**).

When APCs were preloaded with superantigen, the T lymphocyte partially engulfed the APC and produced immunological synapses. In these cell conjugates, ICAM-3 redistributed to the contact region; in some conjugates, the accumulation of ICAM-3 was more evident at the

periphery of the contact region (**Fig. 1a**). The pattern of ICAM-3 redistribution was clearly different from that of the other molecules involved in synapse formation, such as CD3, TCR, CD2, CD28, LFA-1 or ICAM-1 (**Fig. 1** and data not shown). CD3, TCR and CD28 were detected in a small cluster in the center of the synapse (**Fig. 1e–g**), whereas ICAM-1 (in Raji cells) and LFA-1 (in Jurkat cells) were enriched along the contact region (**Fig. 1b,c**), in accordance with published reports[2–5]. The adapter molecule LAT was clustered at the center of the synapse in an antigen-specific manner, but evenly distributed throughout the T cell surface in cell conjugates in the absence of superantigen (**Fig. 1h**).

We determined the redistribution of ICAM-3 in other T cell–APC systems, including the nontransformed, activated human T cell clone S3 (CD4+CD69+CD25+) or resting and activated human peripheral blood lymphocytes (PBLs) in interaction with the lymphoblastoid B cell line LG2 or monocyte-derived DCs (**Fig. 2**). We also determined whether ICAM-3 redistribution to the T cell–APC contact region also occurs in cells that have a polarized distribution of this molecule by studying the interaction of S3 cells with DCs or LG2 cells. In S3 cells, ICAM-3 redistributed to the region of T cell contact with DCs that had been either left untreated or pulsed with staphylococcal enterotoxin B (SEB, **Fig. 2a**).

Notably, the adhesion molecules PSGL-1 and ICAM-3, which colocalize in the uropod of polarized leukocytes[23,24], localized differentially
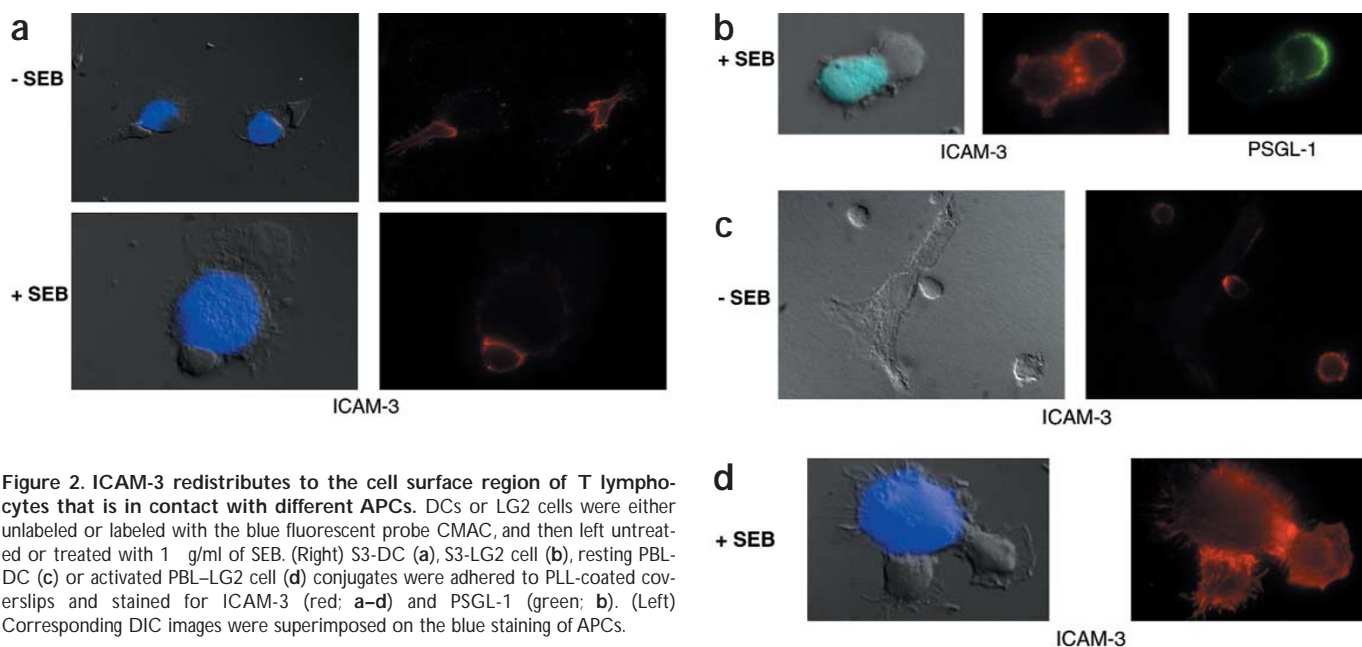
Figure 2. ICAM-3 redistributes to the cell surface region of T lymphocytes that is in contact with different APCs. DCs or LG2 cells were either unlabeled or labeled with the blue fluorescent probe CMAC, and then left untreated or treated with 1 g/ml of SEB. (Right) S3-DC (**a**), S3-LG2 cell (**b**), resting PBL-DC (**c**) or activated PBL–LG2 cell (**d**) conjugates were adhered to PLL-coated coverslips and stained for ICAM-3 (red; **a–d**) and PSGL-1 (green; **b**). (Left) Corresponding DIC images were superimposed on the blue staining of APCs.

to T cell membrane compartments during SEB recognition (**Fig. 2b**). PSGL-1 was not redistributed to the contact site, but actively clustered to the opposite pole of the T cell during SEB recognition in Jurkat-Raji conjugates (**Fig. 1d**). Because ICAM-3 redistribution seemed to be independent of antigen recognition, we studied the interaction of resting human PBLs with DCs. We found that ICAM-3, which was distributed evenly throughout the cell in resting lymphocytes, clustered in the T cell contact region formed with the DC (**Fig. 2c**). We analyzed the localization of ICAM-3 with a polyclonal cell population of SEB-primed PBLs that interact with SEB-treated LG2 cells and found that ICAM-3 also accumulated at the contact region (**Fig. 2d**). These results indicate that ICAM-3 redistributes specifically to the adhesive T cell–APC contact region in both the presence and absence of antigen.

Conjugate formation and ICAM-3 redistribution kinetics
We studied the localization of ICAM-3 during the formation and stabilization of the immunological synapse by following the kinetics of conjugate formation between Jurkat and Raji cells and analyzing the distribution of ICAM-3 in comparison to that of CD3, which is a marker of synapse formation. For quantitative evaluation of the T cell–APC conjugates, we established two morphologically based categories: early conjugates and stabilized conjugates (**Fig. 3a**). ICAM-3 accumulated at the site of T cell–APC interaction in 78±18% of the early conjugates and in 75±14% of the stabilized conjugates (*n*=200); this clustering was independent of SEE recognition (**Fig. 3b**). By contrast, CD3 was concentrated at the center of the synapse in 75±4% of the stabilized conjugates but in only 27±5% of the early conjugates (**Fig. 3b**).

Kinetic studies of conjugate formation showed that the high percentage of early conjugates decreased with time to give rise to stabilized conjugates (**Fig. 3c**). Superantigen accelerated conjugate formation because pretreatment with SEE led to the rapid formation of stable conjugates (within 10 min), which in the absence of superantigen took 40–60 min to form (**Fig. 3c**). We observed a slight reduction in the percentage of stabilized conjugates after 100 min, which might be caused by partial T cell retraction after stabilization of the conjugate—a process in which the T cell acquires a round shape[25] (data not shown);

thus, these complexes were not included in this category. As expected, ICAM-3 was redistributed to the cell-to-cell contact region independently of the presence of superantigen.

The accumulation of ICAM-3 was homogeneous throughout the contact region in some conjugates, but concentrated at the outer zone in others (**Figs. 1** and **2**). We explored the dynamics of ICAM-3 redistribution that underlie this differential localization by analyzing quantitatively the stabilized conjugates in superantigen-driven, polyclonal, activated PBL–LG2 and Jurkat-Raji cell conjugates. Formation of activated PBL–LG2 conjugates coincided with ICAM-3 redistribution to the outer ring, which suggested that there might be a relocation of ICAM-3 to the outer zone of the contact as conjugate stabilization progressed (**Fig. 3d**). But the percentage of conjugates that showed this particular distribution of ICAM-3 was higher in Jurkat-Raji conjugates at earlier time-points (probably because of their larger size), which led to more avid engulfment of the APC and faster stabilization of the conjugate (**Fig. 3d**).

Dynamic redistribution of ICAM-3, PSGL-1 and LAT
We determined the contribution of ICAM-3 to formation of the immunological synapse by comparing the dynamics of ICAM-3 redistribution in T cell–APC conjugates with those of the adhesion molecule PSGL-1 and the T cell signaling molecule LAT. We stably and transiently transfected Jurkat cells with ICAM-3–green fluorescent protein (GFP) and GFP–PSGL-1 constructs to study the dynamic molecular distribution of these adhesion molecules during the T cell–APC interaction. The localization of these molecules was tracked by live-cell time-lapse fluorescence confocal microscopy (**Fig. 4**).

In the absence of superantigen, ICAM-3 accumulated at the site of interaction very rapidly (within the first 30 s) after contact of T lymphocytes with APCs. ICAM-3 redistribution did not preclude the formation of new contacts with another APC where ICAM-3 molecules were also clustered (**Fig. 4a**). All of the initial contacts that gave rise to a stable conjugate were preceded by an accumulation of ICAM-3 (see **Web Movie 1** on the supplementary information page of *Nature Immunology* online). The two
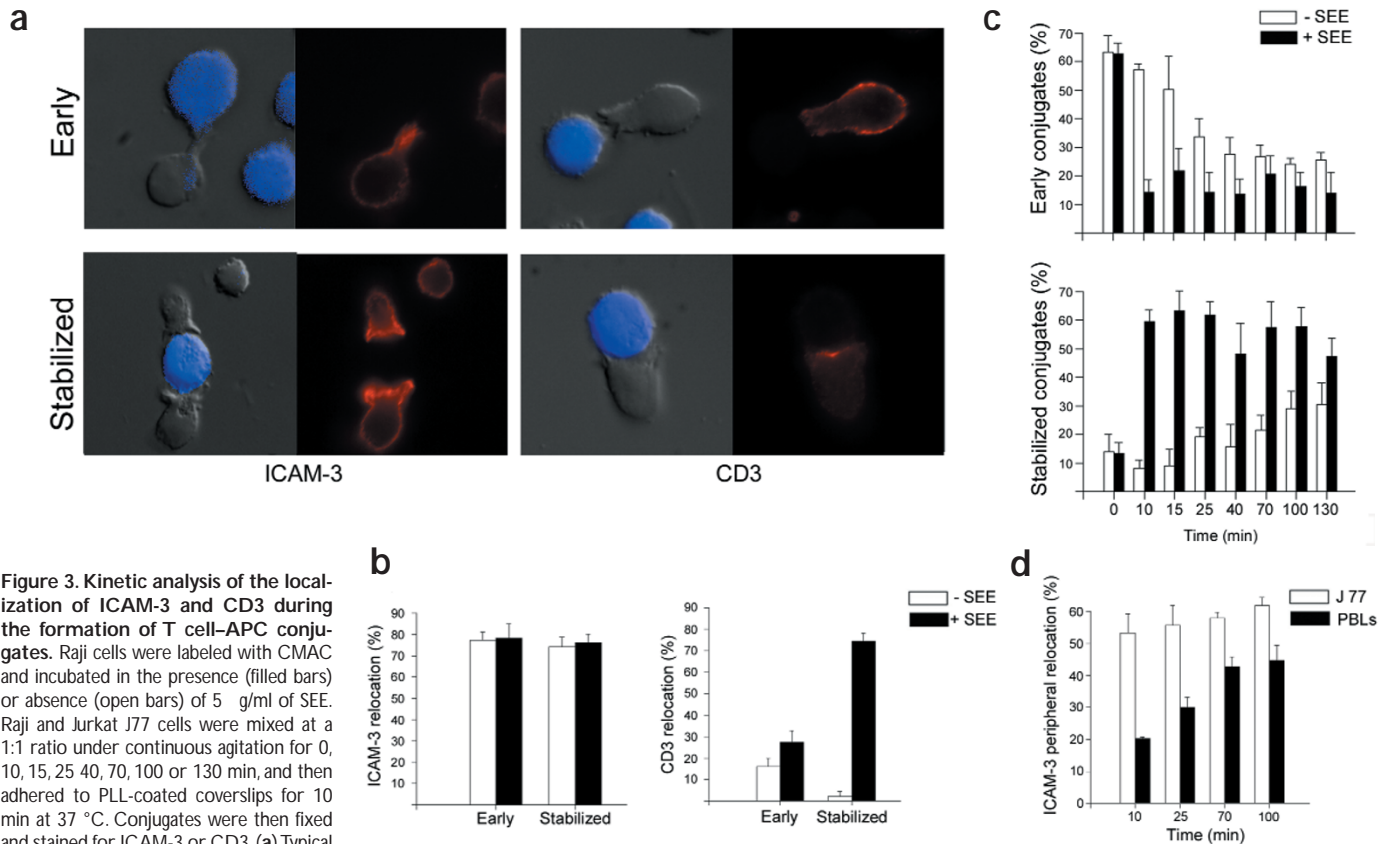
Figure 3. Kinetic analysis of the localization of ICAM-3 and CD3 during the formation of T cell–APC conjugates. Raji cells were labeled with CMAC and incubated in the presence (filled bars) or absence (open bars) of 5 μg/ml of SEE. Raji and Jurkat J77 cells were mixed at a 1:1 ratio under continuous agitation for 0, 10, 15, 25 40, 70, 100 or 130 min, and then adhered to PLL-coated coverslips for 10 min at 37 °C. Conjugates were then fixed and stained for ICAM-3 or CD3. (**a**) Typical examples of early (upper) or stabilized (lower) conjugates. (**b**) Percentage of conjugates with ICAM-3 or CD3 redistributed as shown in **a** relative to the total number of conjugates after 20 min of conjugate formation was determined for the two different categories. (**c**) Percentage of early or stabilized conjugates relative to the total number of conjugates determined at the different times indicated. (**d**) Percentage of stabilized J77-Raji (open bars) or activated PBL–Raji conjugates (filled bars) with ICAM-3 accumulated at the periphery of the contact relative to the total number of stabilized conjugates with ICAM-3 redistributed to the contact determined at the times indicated. Data are mean±s.e.m. of four independent experiments.

punctual contacts between a T cell and an APC that were not followed by ICAM-3 clustering did not lead to the formation of stable conjugates (**Web Movie 1**). Thus, ICAM-3 initiated stable contact between T cells and APCs. In contrast, PSGL-1 did not relocalize to the T cell membrane in the absence of superantigen recognition (**Fig. 4a** and **Web Movie 2**).

We examined the formation of SEE-specific T cell–APC conjugates, which showed that ICAM-3 redistributed rapidly to the site of initial contact and that, on conjugate stabilization, the ICAM-3 accumulated mainly at the outer zone of the cell-cell interface (**Fig. 4b** and **Web Movie 3**). New contacts with additional APCs also resulted in accumulation of ICAM-3 at the contact zone (**Fig. 4b**). After superantigen recognition, PSGL-1 actively accumulated in clusters at the opposite pole of T cell–APC contact region. The redistribution of PSGL-1 was transient and showed slower kinetics compared with ICAM-3 (**Fig. 4b** and **Web Movie 4**). We also studied the dynamic relocation of ICAM-3 in resting PBLs by infecting these cells with a recombinant vaccinia virus that expressed GFP–ICAM-3. ICAM-3 was evenly distributed in these resting PBLs, but redistributed very rapidly to the contact zone on interaction with DCs (**Fig. 4c** and **Web Movie 5**).

To compare the behavior of ICAM-3 with that of a constituent of the immunological synapse, we analyzed stable transfectants of Jurkat $V_\beta 8^+$ T cells expressing LAT fused to GFP. The functional and biochemical behavior of GFP-LAT did not differ from that of endogenous LAT in Jurkat cells, because both proteins were phosphorylated, recruited into

rafts and clustered on the cell surface after stimulation with CD3 (**Fig. 5a–e**). Dynamic analysis showed that LAT did not redistribute in the absence of superantigen stimulation (**Fig 5f** and **Web Movie 6**). LAT redistributed very rapidly to the site of initial interaction with the APC in an antigen-dependent manner and showed redistribution kinetics similar to those observed for ICAM-3, but localized to a different subcellular region. A punctual central cluster appeared 50±6 s after the initial contact of the T cell and the APC. As stabilization of the cell conjugate progressed, the central cluster gave rise to an extended accumulation of LAT throughout most of the contact region 170±20 s after the initiation of the contact, in contrast to the redistribution of ICAM-3 at the edges of the cell-cell interface (**Fig. 5f** and **Web Movie 7**). Thus, ICAM-3, PSGL-1 and LAT show different behavior during the formation of immune synapses: ICAM-3 redistributes selectively on the T cell surface region that initiates contact with the APC before specific antigenic recognition, whereas LAT and PSGL-1 show antigen-driven redistribution to different poles of the T cell.

ICAM-3 in T cell–APC conjugate formation

The relocation of ICAM-3 to the APC contact zone indicated that this molecule might be involved in initiating adhesive events that lead to APC recognition by T lymphocytes. We examined the functional role of ICAM-3 in this process by studying the effect of pretreating Jurkat cells or resting PBLs with blocking ICAM-3 antibodies and by analyzing the formation of conjugates with Raji cells that were either pulsed with SEE or not.
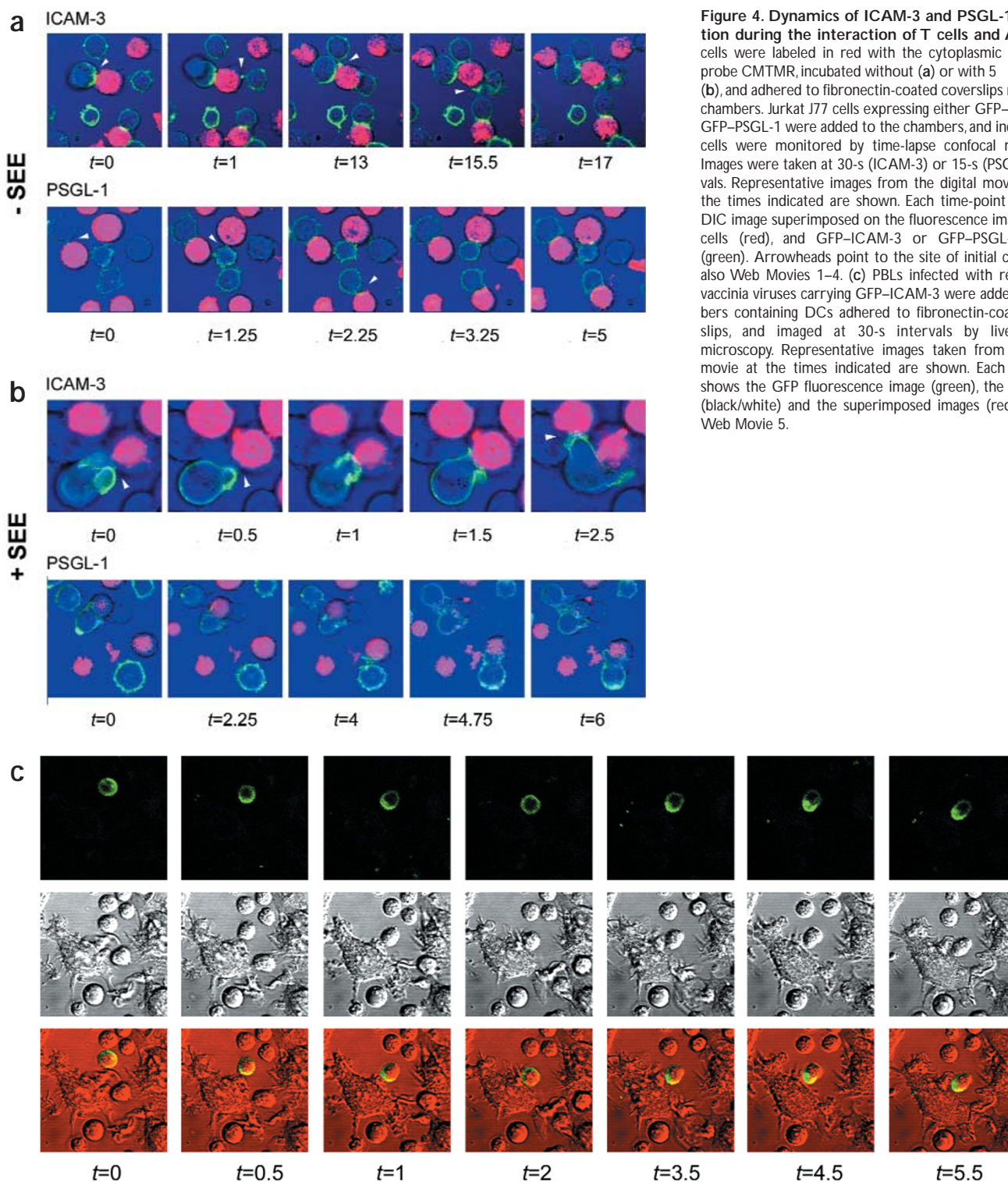
Figure 4. Dynamics of ICAM-3 and PSGL-1 distribution during the interaction of T cells and APCs. Raji cells were labeled in red with the cytoplasmic fluorescent probe CMTMR, incubated without (**a**) or with 5 g/ml of SEE (**b**), and adhered to fibronectin-coated coverslips mounted in chambers. Jurkat J77 cells expressing either GFP–ICAM-3 or GFP–PSGL-1 were added to the chambers, and individual live cells were monitored by time-lapse confocal microscopy. Images were taken at 30-s (ICAM-3) or 15-s (PSGL-1) intervals. Representative images from the digital movie taken at the times indicated are shown. Each time-point shows the DIC image superimposed on the fluorescence images of Raji cells (red), and GFP–ICAM-3 or GFP–PSGL-1 staining (green). Arrowheads point to the site of initial contact. See also Web Movies 1–4. (**c**) PBLs infected with recombinant vaccinia viruses carrying GFP–ICAM-3 were added to chambers containing DCs adhered to fibronectin-coated coverslips, and imaged at 30-s intervals by live confocal microscopy. Representative images taken from the digital movie at the times indicated are shown. Each time-point shows the GFP fluorescence image (green), the DIC image (black/white) and the superimposed images (red). See also Web Movie 5.

Conjugate formation in the absence of superantigen recognition was inhibited by anti–ICAM-3 but not by blocking anti–LFA-1 or anti–ICAM-1 (**Fig. 6a**). But both anti–LFA-1 and anti–ICAM-3 blocked the formation of superantigen-specific T cell–APC conjugates (**Fig. 6a**), in accordance with the reported role of LFA-1 in stabilizing the immunological synapse[1].

The blocking ICAM-1 antibody did not show any effect on conjugate formation (**Fig. 6a**), probably owing to the low expression of ICAM-1

in these cells (**Fig. 1b** and data not shown). As a control, we also examined the effect of blocking VLA-4 antibodies, which did not affect T cell–APC conjugate formation (data not shown). We quantified the inhibition of superantigen-driven conjugate formation by anti–ICAM-3 on PBLs interacting with Raji cells in kinetic assays. The inhibition after 20, 60 and 120 min of conjugate formation was 51.8±7.4%, 56±5.6% and 49.4±12%, respectively, which indicates that inhibition
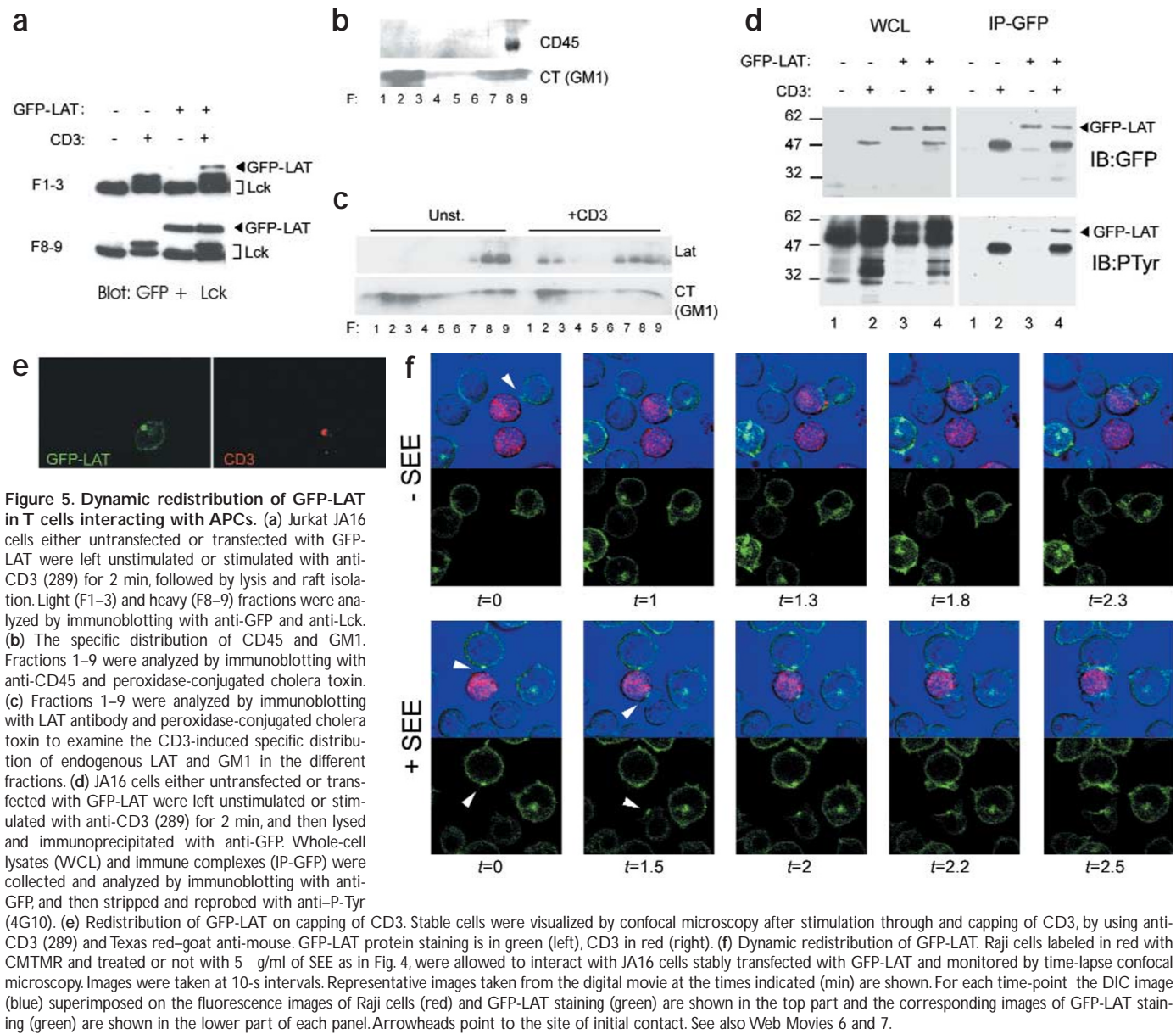
Figure 5. Dynamic redistribution of GFP-LAT in T cells interacting with APCs. (a) Jurkat JA16 cells either untransfected or transfected with GFP-LAT were left unstimulated or stimulated with anti-CD3 (289) for 2 min, followed by lysis and raft isolation. Light (F1–3) and heavy (F8–9) fractions were analyzed by immunoblotting with anti-GFP and anti-Lck. (b) The specific distribution of CD45 and GM1. Fractions 1–9 were analyzed by immunoblotting with anti-CD45 and peroxidase-conjugated cholera toxin. (c) Fractions 1–9 were analyzed by immunoblotting with LAT antibody and peroxidase-conjugated cholera toxin to examine the CD3-induced specific distribution of endogenous LAT and GM1 in the different fractions. (d) JA16 cells either untransfected or transfected with GFP-LAT were left unstimulated or stimulated with anti-CD3 (289) for 2 min, and then lysed and immunoprecipitated with anti-GFP. Whole-cell lysates (WCL) and immune complexes (IP-GFP) were collected and analyzed by immunoblotting with anti-GFP, and then stripped and reprobed with anti–P-Tyr (4G10). (e) Redistribution of GFP-LAT on capping of CD3. Stable cells were visualized by confocal microscopy after stimulation through and capping of CD3, by using anti-CD3 (289) and Texas red–goat anti-mouse. GFP-LAT protein staining is in green (left), CD3 in red (right). (f) Dynamic redistribution of GFP-LAT. Raji cells labeled in red with CMTMR and treated or not with 5 μg/ml of SEE as in Fig. 4, were allowed to interact with JA16 cells stably transfected with GFP-LAT and monitored by time-lapse confocal microscopy. Images were taken at 10-s intervals. Representative images taken from the digital movie at the times indicated (min) are shown. For each time-point the DIC image (blue) superimposed on the fluorescence images of Raji cells (red) and GFP-LAT staining (green) are shown in the top part and the corresponding images of GFP-LAT staining (green) are shown in the lower part of each panel. Arrowheads point to the site of initial contact. See also Web Movies 6 and 7.

was sustained. These results confirmed that ICAM-3 is essential for the initial phase of conjugate formation.

Because ICAM-3 ligands such as DC-SIGN are not expressed in the Raji B cell line (data not shown), we determined whether LFA-1 was the ligand of ICAM-3 on these cells by blocking experiments. Preincubating Raji cells with Fab fragments of blocking anti–LFA-1 (TS1/18) produced 7.6±1.1% of antigen-nonspecific conjugate formation. Control preincubations using Fab fragments of anti–HLA MHC class I (W6/32) or anti-CD9 (VJ1/10) produced a conjugate formation of 15.2±1.7 and 17.6±1.2%, respectively. The significant anti–LFA-1–mediated inhibition of conjugate formation (53.6±7.4% inhibition; Student's t-test, P<0.05) indicates that LFA-1 is the principal ICAM-3 receptor in this T cell–APC system.

Regulatory role of ICAM-3 in early TCR signaling

To investigate further the functional role of ICAM-3 in initial T cell–APC interactions, we tested whether ICAM-3 could act as a costimulatory molecule in early signaling events triggered by the TCR. Jurkat cells expressing GFP-LAT were exposed to suboptimal doses of anti-CD3 and activating ICAM-3 or CD28 monoclonal antibodies (mAbs), which induced tyrosine phosphorylation of LAT to a similar extent as treatment with optimal doses of anti-CD3 (**Fig. 6b**). Similar results were obtained when we used dephosphorylation of NFAT as a parameter of T cell activation. The ICAM-3 mAb (HP2/19), in combination with suboptimal doses of anti-CD3, reduced phosphorylated NFAT in Jurkat cells to amounts comparable to those obtained with the Ca^{2+} ionophore A23187, an optimal dose of CD3, or the combination of suboptimal doses of CD3 and CD28 antibodies (**Fig. 6c**). Anti–ICAM-3 alone, however, did not exert any effect on LAT or NFAT phosphorylation. As a control, we pretreated the cells with the immunosuppressive drug cyclosporin A (CsA), which inhibits the phosphatase activity of calcineurin—the kinase that dephosphorylates NFAT; pretreatment with CsA completely abolished the anti-CD3 effect (**Fig. 6c**).
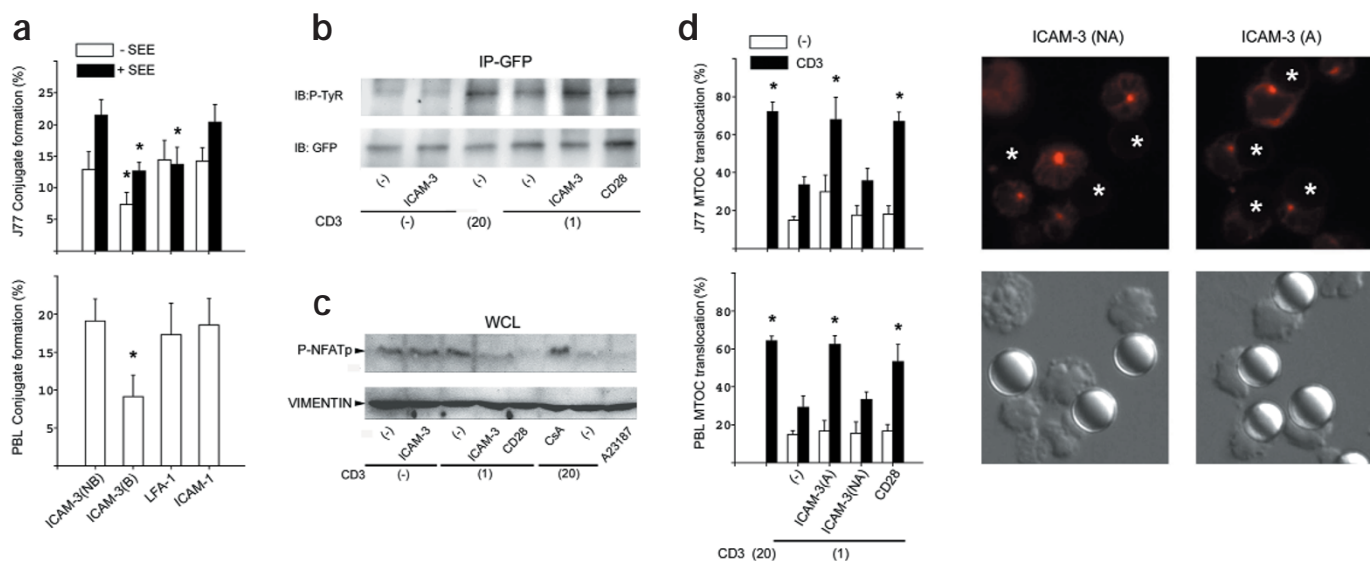
Figure 6. Functional role of ICAM-3 in conjugate formation, regulation of LAT and NFAT phosphorylation, and MTOC translocation. (a) Jurkat J77 cells or PBLs were preincubated with 20 μg/ml of blocking (B) anti–ICAM-3 (140-11), anti–ICAM-1 (Hu5/3) or anti–LFA-1 (TS1/18), or the nonblocking (NB) anti–ICAM-3 (TP1/24) before conjugation with CMAC-labeled Raji cells that had been pulsed with SEE (filled bars) or not (open bars). Conjugation was assessed after 20 min. Data are mean±s.e.m. of six independent experiments. Bars represent the mean conjugate formation relative to the number of Raji cells (*P<0.05, Student's t-test). (b) GFP-LAT–transfected Jurkat JA16 cells were either left unstimulated (–) or stimulated with anti-CD3 (T3b) at optimal (20 μg/ml) or suboptimal (1 μg/ml) doses, in the presence of 20 μg/ml of anti–ICAM-3 (HP2/19) or anti-CD28 (CD28.2) for 2 min at 37 °C. Immune complexes obtained with anti-GFP were analyzed by immunoblotting with anti-P-Tyr (P-Tyr; 4G10), and then stripped and reprobed with anti-GFP (GFP). (c) Jurkat J77 cells were stimulated with or without optimal (20 μg/ml) or suboptimal (1 μg/ml) doses of anti-CD3 (T3b), in the presence of 20 μg/ml anti–ICAM-3 (HP2/19) or anti-CD28 (CD28.2) for 20 min at 37 °C. Where indicated, cells were pretreated with 1 μg/ml of CsA or 1 μM Ca²⁺ ionophore A23187. Equal amounts of whole-cell lysates (WCL) were collected and analyzed by immunoblotting with antiserum specific for NFATp. As loading controls, blots were stripped and reprobed with anti-vimentin. (d) J77 cells or PBLs were mixed at a 1:1 ratio with latex beads either coated (filled bars) or not (open bars) with anti-CD3 (T3b) at optimal (20 μg/ml) or suboptimal (1 μg/ml) doses, and/or activating anti–ICAM-3 (20 μg/ml HP2/19; A) or nonactivating anti–ICAM-3 (20 μg/ml TP1/24; NA), or anti-CD28 (CD28.2). After 15 min, conjugates were adhered to PLL-coated coverslips, fixed and stained with anti–α-tubulin, and scored for MTOC reorientation by direct visualization of fluorescence and bright field images. Data are mean±s.e.m. of four independent experiments. Bars represent the mean MTOC translocation relative to the number of J77-bead conjugates (*P<0.05, Student's t-test). Representative images of J77 conjugates with beads coated with control nonactivating anti–ICAM-3 (TP1/24; NA), or the activating anti–ICAM-3 (HP2/19; A) plus a suboptimal concentration of anti-CD3 (1 μg/ml) are shown. Upper panels show staining for α-tubulin; lower panels show the corresponding DIC images. Asterisks indicate the position of the bead in the fluorescence image

We analyzed the effects of ICAM-3–mediated regulation of early signaling by studying cytoskeletal rearrangements using antibody-coated microspheres as artificial APCs[26]. As a positive control, we incubated Jurkat T cells or PBLs with beads coated with optimal doses of anti-CD3 that strongly induced MTOC reorientation to the contact region with the microsphere. When suboptimal doses of anti-CD3 were used, only a weak effect on MTOC reorientation was observed with respect to the negative control (**Fig. 6d**). Microspheres coated with anti–ICAM-3 or anti-CD28 did not induce a reorientation of MTOC; however, the combination of a suboptimal dose of anti-CD3 with the stimulatory ICAM-3 mAb HP2/19[17] induced MTOC reorientation to a similar extent as that obtained with either costimulation by CD28 or the optimal dose of anti-CD3 (**Fig. 6d**). In contrast, the control, nonactivating ICAM-3 mAb TP1/24[17], alone or in combination with suboptimal doses of anti-CD3, did not exert this effect (**Fig. 6d**). Thus, ICAM-3 can induce a costimulatory effect on early TCR-mediated signaling events, which leads to polarization of the microtubular cytoskeleton.

Discussion

Low-affinity adhesive interactions facilitate the exploration of the APC surface by T cells. Although this is a key event in initiating the immune response, the molecules responsible for establishing the T cell–APC interaction have remained elusive. LFA-1 is expressed on the surface of resting T lymphocytes in an inactive state that prevents unspecific interactions[27]. Thus, adhesion mediated by LFA-1 requires prior activation,

which is induced by intracellular signals generated through cell surface receptors such as TCR-CD3 and CD2[28,29]. In the current model of T cell–APC interaction[1], LFA-1 is activated by chemokines that mediate the initial antigen-independent adhesion.

Despite increasing evidence to suggest that ICAM-3 has a role in the early adhesive interactions between T cells and APCs, no direct evidence supporting this hypothesis has been reported. We have shown here that a characteristic clustering of ICAM-3 occurs in the region of the T cell surface that is in contact with the APC by using a polyclonal population of resting and activated T lymphocytes (PBLs), the nontransformed activated human CD4 T cell clone (S3) and Jurkat T cells. We have shown that a functional immunological synapse is formed *via* the above model of superantigen-driven T cell–APC conjugate formation[1]. The clustering of endogenous ICAM-3 at cell-cell contacts occurred in both antigen-independent and antigen-dependent T cell–APC interactions. This clustering occurred very rapidly after the initial cell-cell contact, which supports the idea that ICAM-3 is involved in early adhesive events. Accordingly, both kinetic and dynamic studies show that ICAM-3 is concentrated in the early contact but later redistributes to the outer zone of the contact region.

Under conditions of specific antigen recognition, the exclusion of ICAM-3 from the synapse could be directed by lipid-raft-dependent motion[30,31] or by size segregation[32]. In this regard, a fraction of ICAM-3 molecules localizes to the membrane rafts of polarized lymphocytes[33]. Here, ICAM-3 and LAT showed different patterns of redistribution,

which highlights the different roles that these molecules have in T cell–APC interactions. The association of LAT with lipid rafts is necessary for its signaling function[34–36]. We found that LAT concentrated in a single cluster at the center of the interface between the T cell and the APC and that this punctual cluster subsequently gave rise to a more diffuse distribution throughout the T cell–APC interface. Accordingly, CD4, which interacts with LAT[37], is initially clustered to the central SMAC and then moves to the periphery[38]. The differential redistribution of CD4-LAT and ICAM-3 might reflect raft dynamics at the T cell–APC contact region. There is increasing evidence that lipid rafts are small membrane domains of 50–100 nm[12], and are heterogeneous across different subcellular membrane compartments[39]. On antigen recognition, CD4-LAT and ICAM-3–containing rafts might be segregated differently at T cell–APC interface to perform different functions. Alternatively, the differential redistribution might be due to the distinct ability of CD4-LAT and ICAM-3 to be localized in (or delocalized from) rafts under TCR stimulation.

We found that ICAM-3 and PSGL-1, which colocalize in the uropod of polarized leukocytes[23,24], were located in opposite poles of the T cells interacting with APCs. The clustering of PSGL-1 to the opposite pole of the T cell–APC contact region was observed only on superantigen-specific recognition and occurred during engulfment of the APC, which has been related to the peak of Ca^{2+} rise in T lymphocytes[25]. Antigen-dependent active exclusion from the T cell–APC interface has been also described for CD43, another member of the family of mucin-like molecules[40]. The exclusion of PSGL-1 and CD43 from the interaction site might be due to their large size and highly glycosylated nature, which could hamper membrane apposition; however, the exact mechanism is unclear at present. Our time-lapse studies showed that ICAM-3 accumulation at the site of interaction preceded the clustering of PSGL-1 at the opposite pole. Because the actin-linking proteins ezrin and moesin interact with ICAM-3 and PSGL-1, and are involved in their redistribution toward the uropod in migrating lymphocytes[24,41], they might also be involved in the differential subcellular targeting of ICAM-3 and PSGL-1 during immune cell-cell interactions. But how the association or dissociation of these membrane receptors from ezrin and moesin is regulated is unknown.

The role of ICAM-3 in initiating the adhesive interactions of T cells with APCs was shown directly by the inhibition of conjugate formation when T lymphocytes were pretreated with anti–ICAM-3. In antigen-nonspecific conjugates, anti–ICAM-3 had a blocking effect on T cells, whereas anti–ICAM-1 and anti–LFA-1 were ineffective. These results support the idea that ICAM-3 has a predominant role in the early T cell–APC interactions. In contrast, the partial inhibitory effect of ICAM-3 antibodies is in accordance with their incomplete blockade of other ICAM-3–mediated cellular functions[42]. Inhibition of antigen-independent conjugate formation was achieved when APCs, but not T cells, were preincubated with a blocking LFA-1 antibody, which indicates that LFA-1 is the principal adhesion ligand for ICAM-3 on Raji cells, as these cells lack expression of DC-SIGN[21]. Our finding that anti-ICAM-3 inhibited the formation of T cell–APC conjugates explains previous observations in which anti–ICAM-3 reduced T cell proliferation in DC-stimulated primary mixed lymphocyte reactions[43–45].

The costimulatory activity of ICAM-3 has been described[16–19]. The clustering of ICAM-3 in the contact region also influenced early TCR-triggered signaling events that lead to T cell activation, such as LAT phosphorylation and NFAT dephosphorylation. In addition, ICAM-3 could transduce early signals that lead to polarization of intracellular components, such as reorienting the MTOC towards the contact with the activating interface. In summary, our data indicate

that ICAM-3 functions as a primary adhesion molecule during initiation of adhesive contact that occurs between T cells and APCs before antigen recognition.

Methods

Cells, antibodies and reagents. The T cell lines Jurkat J77cl20 (J77)[22] and JA16, and the lymphoblastoid B cell lines Raji and LG2 were cultured in RPMI-1640 medium with 10% fetal calf serum (FCS, Gibco-BRL, Gaithersburg, MD). We generated polyclonal SEB-activated PBLs and the CD4 T cell clone S3085B (S3) by incubating irradiated LG2 cells and peripheral blood monocytes in medium supplemented with 0.5 g/ml of SEB and 50 U/ml of human recombinant IL-2. Cells were restimulated every 2 weeks as described[46]. The S3 clone was generated by limiting dilution. Human PBLs were isolated from fresh blood using a Ficoll-Hypaque density gradient. We obtained DCs as described[47]. Briefly, we cultured peripheral blood monocytes in the presence of IL-4 and granulocyte–macrophage colony-stimulating factor (10 g/ml and 1000 U/ml, respectively) and after 5 days added tumor necrosis factor-α (10 ng/ml) to the culture media. We confirmed the phenotype of mature DCs (CD80hiCD83hiCD14lo) by flow cytometric analysis.

We used the following mouse anti-human mAbs (all from Sigma, St Louis, MO): W6/32 (anti–HLA class I); VJ1/10 (anti-CD9); TP1/24, HP2/19 (anti–ICAM-3)[42]; 289.1 (anti-CD3); 4G1.5 (anti–V$_\beta$8 TCR); T3b (anti-CD3); TS1/18 (anti–β$_2$)[48]; CD28.2 (anti-CD28)[49]; PL-1 (anti–PSGL-1)[24]; DM1A (anti–α-tubulin). Anti–ICAM-3 (140.11) was from R. Vilella (Hospital Clinic, Barcelona, Spain) and anti-NFATp (672)[50] from J. M. Redondo (Centro de Biología Molecular, Madrid, Spain). Rabbit polyclonal anti-LAT and anti–P-Tyr 4G10 were from Upstate Biotechnology (Lake Placid, NY); anti-CD80, anti-CD83 and anti-CD14 were from Becton Dickinson (San Jose, CA); and anti-GFP (290) was from Abcam (Cambridge, UK). Anti-vimentin, recombinant human fibronectin, poly(L)lysine (PLL), geneticin, Cyclosporin A, ionophore A23187 and SEB were from Sigma. We obtained SEE from Toxin Technology (Sarasota, FL). The fluorescent cell trackers chloromethyl derivative of aminocoumarin (CMAC), chloromethylbenzoylaminotetramethylrhodamine (CM-TMR), calcein and hydroethidin were from Molecular Probes (Eugene, OR), and human recombinant IL-2 (Hoffmann-LaRoche, Nutley, NJ) was from the NIH AIDS Research and Reference Reagent program.

Expression of recombinant DNA constructs. We generated GFP-ICAM-3, GFP–PSGL-1 and GFP-LAT by using human ICAM-3, PSGL-1 and LAT cDNAs as templates from which we amplified the complete coding region of these molecules by polymerase chain reaction (PCR). The PCR products were subcloned into pEGFP-N1 (ICAM-3 and PSGL-1) or pEGFP-N3 (LAT, Clontech, Palo Alto, CA), which resulted in an in-frame fusion of enhanced GFP (EGFP) to the COOH-terminus of ICAM-3 and PSGL-1, or to the NH$_2$-terminus of LAT. The EGFP–ICAM-3 fusion protein cDNA was then excised from the ICAM-3–pEGFP-N1 plasmid and subcloned into the pRB21 plasmid (from J. A. Melero, Instituto de Biología Fundamental, Instituto de Salud Carlos III, Madrid, Spain). The resultant GFP–ICAM-3–pRB21 vector was inserted into the defective vRB12 strain of vaccinia virus by homologous recombination. We generated transiently transfected Jurkat cells by electroporation and used these cells 24 h later after eliminating dead cells by centrifugation over a Ficoll-Hypaque gradient. V$_\beta$8-expressing Jurkat J77 or JA16 cells were stably transfected with GFP–ICAM-3 and GFP–PSGL-1 or GFP-LAT, respectively. Stable clones were obtained by sorting stably transfected cells selected with growing media containing 0.5 mg/ml of geneticin for 2 weeks.

Conjugate formation and immunofluorescence. To distinguish APCs from T lymphocytes, we loaded Raji, LG2 and DCs with the blue fluorescent cell tracker CMAC. Briefly, cells were preincubated in Hanks balanced salt solution (HBSS) containing 10 M CMAC for 20 min at 37 °C, washed and resuspended (5 10^6 cells/ml) in HBSS. The cells were then incubated for 20 min in the presence or absence of 5 g/ml of SEE (Raji) or 1 g/ml of SEB (LG2 and DC). We mixed J77, S3 T cells or PBLs (5 10^4 cells/well) with an equal number of Raji, LG2 or DCs (2 10^4 cells/well) in a final volume of 600 l and immediately plated them onto PLL-coated slides in flat-bottomed 24-well plates (Costar Corporation, Corning, NY). For kinetics analyses, J77 and Raji cells or activated PBLs and Raji cells were mixed and incubated for the indicated times under continuous rotation in a final volume of 600 l. Conjugates were either centrifuged on the plates and then immediately fixed (0 min) or allowed to settle for additional 10 min at 37 °C, fixed for 5 min in 4% formaldehyde-PBS, and stained with the appropriate antibodies, using goat anti-mouse rhodamine red X as secondary antibody (Molecular Probes) as described[23]. We observed cells by a DMR photomicroscope (Leica, Mannheim, Germany) with 63 and 100 oil immersion objectives. Images were acquired using the Leica QFISH 1.0 software.

We analyzed cell conjugate formation quantitatively by fluorescence microscopy. Conjugates were first identified by directly observing both cell morphology under differential interference contrast (DIC) and blue-fluorescent CMAC-labeled APCs. The proportion of conjugates with ICAM-3 or CD3 redistributed to the cell-cell contacts was calculated by randomly choosing 200 different conjugates and identifying which of these had an accumulation of the fluorescent signal at the contact region. Two categories of conjugates were established according to morphology parameters: early and stabilized conjugates (**Fig. 3a**). We identified and assigned conjugates to the different categories directly under the fluorescence microscope. Conjugates with other morphologies, such as those that had not undergone complete stabilization (intermediate) and those in which the T cell had retracted after stabilization, were not included in these categories.

For antibody blocking studies, J77 cells or PBLs were preincubated with the appropriate antibodies (20 g/ml) for 30 min at 4 °C. Raji cells were preincubated with Fab fragments (60 g/ml) of the appropriate antibodies for 30 min at 4 °C. We allowed T cells to interact with Raji cells for 5 min at 30 °C under continuous agitation in HBSS plus 2% FCS. The proportion of conjugates was calculated by randomly choosing 20 different fields (63 objective) of each condition and determining the number of conjugates relative to the total number of Raji cells in each field. We counted a minimum of 100 conjugates for each condition.

Time-lapse fluorescence confocal microscopy. We coated coverslips with fibronectin (20 g/ml) for 20 h at 4 °C, and saturated them with HBSS containing 1% bovine serum albumin (BSA) for 30 min at 37 °C. Thereafter, coverslips were washed with HBSS and mounted in Attofluor open chambers (Molecular Probes) and placed on the microscope stage. We allowed 6 × 10⁵ J77 cells or DCs in 500 l of HBSS containing 2% FCS to adhere on these chambers for 30 min. Raji cells (2 × 10⁵) previously incubated with 5 M CM-TMR for 20 min at 37 °C, or PBLs (5 × 10⁵) resuspended in HBSS plus 2% FCS were added to the chamber containing the adhered J77 or DCs, and maintained at 37 °C in a 5% CO₂ atmosphere. Confocal images were acquired using a Leica TCS-SP confocal laser scanning unit equipped with Ar and He-Ne laser beams and attached to a Leica DMIRBE inverted epifluorescence microscope. We obtained serial fluorescence and DIC images simultaneously at the indicated intervals. Optical sectioning was necessary to capture all of the green fluorescent signal. The most representative section of the green channel (GFP signal), its corresponding DIC image (which provides information about the morphology of the cell), and the image from the red channel, which shows the staining for Raji cells (CM-TMR signal), were overlaid in a single image. We used either the 63 or 100 objectives, and processed and assembled the images into movies using Leica confocal software.

Lipid raft isolation and immunoblotting. Fresh stable cell lines (3 × 10⁷ cells), stimulated or not with anti-CD3 (289.1) were sonicated gently in 1 ml of ice-cold buffer A (25 mM Tris, pH 7.5, 150 mM NaCl, 5 mM EDTA) supplemented with a mixture of protease inhibitors (1 g/ml of leupeptin, 1 g/ml of pepstatin, 2 g/ml of chymostatin and 5 g/ml of α₂ macroglobulin). After centrifugation at 800g at 4 °C for 10 min, the post-nuclear supernatant (PNS) was incubated with 1% Brij 98 for 4 min at 37 °C with gentle shaking. We adjusted the lysate to 1.33 M sucrose by adding 2 ml 2 M sucrose in buffer A, and placed it at the bottom of an ultracentrifuge tube. A sucrose gradient (0.2–0.9 M in 0.1-M steps of 1 ml) in buffer A was placed on top and the tube was centrifuged at 38,000 rpm for 16 h at 4 °C. Lipid rafts were mainly recovered from low-density fractions 1, 2 and 3 (F1–3); fractions 8 and 9 (F8–9) corresponded to the bottom fractions.

For phosphotyrosine (P-Tyr) protein analysis, buffer A was supplemented with 1 mM NaVO₄, 10 mM sodium pyrophosphate and 10 mM NaF. After SDS-PAGE on 7–17% gradient polyacrylamide gels, proteins were transferred onto polyvinylidene difluoride (PVDF) membranes (Millipore, Bedford, MA). Blots were then incubated with anti–P-Tyr (4G10) and the appropriate horseradish peroxidase (HRP)-conjugated secondary antibody. We detected EGFP fusion proteins by using the anti-GFP stabilized antibody preparation—a mixture of two mouse mAbs (7.1 and 13.1; Roche Boehringer Mannheim, Indianapolis, IN). CD45 and Lck were detected using mouse mAbs from Transduction Labs (Lexington, KY) and Santa Cruz Biotechnology (Santa Cruz, CA), respectively, and GM1 was detected using peroxidase-conjugated cholera toxin (CT) from Sigma. LAT was revealed using a polyclonal serum from immunized rabbits (J. Nunes et al., unpublished data).

Immunoprecipitation. The JA16 cells (10⁷) were either left unstimulated or stimulated by anti-CD3 (289.1, 10 g/ml) for 2 min at 37 °C. The cells were then washed once in PBS and lysed for 20 min at 4 °C in NTE buffer (150 mM NaCl, 25 mM Tris, pH 7.8, 5 mM EDTA) supplemented with 1% Nonidet P-40 plus protease and phosphatase inhibitors. After being lysed, postnuclear supernatants were collected by centrifugation, and the GFP fusion protein was immunoprecipitated using polyclonal anti-GFP from Abcam (Ab 290) and protein A Sepharose. After being washed extensively in lysis buffer, the immune complexes were analyzed by immunoblotting.

Capping. We washed and resuspended stable cell lines (10⁶ cells) in 500 l of PBS, and added anti-CD3 (289.1, 10 g/ml) for 30 min at 4 °C. The cells were then washed, resuspended in 500 l of PBS plus 0.2% BSA and incubated for 30 min in the presence of a Texas red–goat anti-mouse (Molecular Probes). This protocol allowed the cells to undergo simultaneous stimulation and CD3 capping. We washed the cells in PBS, 5% FCS and 0.1% sodium azide, fixed them in 2% paraformaldehyde for 30 min at room temperature, washed them in PBS, and then transferred them onto silane-treated glass slides (3-aminopropyltriethoxysilane; Sigma) for visualization under a TCS NT confocal microscope (Leica).

Costimulation experiments. The JA16 cells (10⁷) were washed and resuspended in 300 l of RPMI medium, and anti-CD3 (T3b) was added at the doses indicated. Anti ICAM-3 (HP2/19; 20 g/ml) or anti-CD28 (CD28.2; 20 g/ml) was added where indicated, and the cells were incubated for 15 min at 4 °C. We then added a sheep anti–mouse IgG (10 g/ml) and incubated the cells for 2 min at 37 °C. After this period, we carried out the immunoprecipitation protocol described above. Immune complexes of GFP-LAT were analyzed by immunoblotting. For NFATp phosphorylation analyses, J77 cells were treated as indicated above for JA16 cells, and incubated for 20 min at 37 °C. The Ca²⁺ ionophore A23187 (1 M final concentration) was included where indicated. For the CsA control, cells were pretreated with 1 g/ml of CsA at 37 °C for 30 min. Cells were lysed in TBS plus 0.5% Triton X-100 supplemented with protease inhibitors for 30 min on ice. Postnuclear supernatants

were collected, run on SDS-PAGE gels and transferred to PVDF membranes. Blots were then incubated with the anti-NFATp and anti-vimentin, and the appropriate HRP-conjugated secondary antibody.

MTOC translocation assays. Antibody-coated beads were made as described[26]. In brief, we incubated 10⁷ styrene beads (6.4 m diameter; Sigma) for 90 min at room temperature with a suboptimal (1 g/ml) or optimal (20 g/ml) concentration of anti-CD3, anti–ICAM-3 (HP2/19 or TP1/24, 20 g/ml) or anti-CD28 (CD28.2, 20 g/ml) under continuous rotation. Beads were then saturated with HBSS plus 1% BSA, washed and stored at 4 °C until use. For conjugation assays, J77 cells or PBLs and antibody-coated beads were mixed at a 1:1 ratio in medium and allowed to interact for 15 min at 37 °C. We gently resuspended the conjugates and plated them onto PLL-coated coverslips for 30 min. The cells were then fixed and permeabilized for 5 min in PBS, 0.5% Triton X-100 and 2% formaldehyde, and stained with anti–α-tubulin (DM1A). When samples were visualized under the fluorescence microscope, the beads appeared round and refringent. We scored the MTOC as reoriented if it was located in close proximity to the T cell plasma membrane between the nucleus and the bead contact region. We scored at least 200 conjugates in each experiment.

Note: Supplementary information can be found on the Nature Immunology *website (http://immunology.nature.com/supp_info/).*

1. Dustin, M. L. & Chan, A. C. Signaling takes shape in the immune system. Cell 103, 283–294 (2000).
2. Monks, C. R. F., Kupfer, H., Tamir, I., Barlow, A. & Kupfer, A. Selective modulation of protein kinase C-θ during T cell activation. Nature 385, 83–86 (1997).
3. Monks, C. R. F., Freiberg, B. A., Kupfer, H., Sclaky, N. & Kupfer, A. Three-dimensional segregation of supramolecular activation clusters in T cells. Nature 395, 82–86 (1998).
4. Dustin, M. L. et al. A novel adaptor protein that orchestrates receptor patterning and cytoskeletal polarity in T-cell contacts. Cell 94, 667–677 (1998).
5. Grakoui, A. et al. The immunological synapse: a molecular machine controlling T cell activation. Science 285, 221–227 (1999).
6. van-der-Merwe, P. A., Davis, S. J., Shaw, A. S. & Dustin, M. L. Cytoskeletal polarization and redistribution of cell surface molecules during T cell antigen recognition. Semin. Immunol. 12, 92–98 (2000).
7. Kupfer, A. & Singer, S. J. Cell biology of cytotoxic and helper T cell functions: immunofluorescence microscopic studies of single cells and cell couples. Annu. Rev. Immunol. 7, 309–337 (1989).
8. Iwashima, M., Irving, B. A., van-Oers, N. S. C., Chan, A. C. & Weiss, A. Sequential interactions of the TCR with two distinct cytoplasmic tyrosine kinases. Science 263, 1136–1139 (1994).
9. van-Oers, N. S., Killeen, N. & Weiss, A. Lck regulates the tyrosine phosphorylation of the T cell receptor subunits and ZAP-70 in murine thymocytes. J. Exp. Med. 183, 1053–1062 (1996).
10. Zhang, W., Sloane-Caster, J., Kitchen, J., Trible, R. P. & Samelson, L. E. LAT: the ZAP-70 tyrosine kinase substrate that links T cell receptor to cellular activation. Cell 92, 83–92 (1998).
11. Law, C. L. et al. GrpL, a Grb2-related adaptor protein, interacts with SLP-76 to regulate nuclear factor of activated T cell activation. J. Exp. Med. 189, 1243–1253 (1999).
12. Simons, K. & Toomre, D. Lipid rafts and signal transduction. Nature Rev. Mol. Cell Biol. 1, 31–39 (2000).
13. de-Fougerolles, A. R., Qin, X. & Springer, T. A. Characterization of the function of intercellular adhesion molecule ICAM-3 and comparison with ICAM-1 and ICAM-2 in immune responses. J. Exp. Med. 179, 619–629 (1994).
14. Fawcett, J. et al. Molecular cloning of ICAM-3 a third ligand for LFA-1, constitutively expressed on resting leukocytes. Nature 360, 481–484 (1992).
15. de-Fougerolles, A. R. & Springer, T. A. Intercellular adhesion molecule 3, a third adhesion counter-receptor for lymphocyte function-associated molecule 1 on resting lymphocytes. J. Exp. Med. 175, 185–190 (1992).
16. Hernandez-Caselles, T. et al. ICAM-3, the third LFA-1 counterreceptor, is a co-stimulatory molecule for both resting and activated T lymphocytes. Eur. J. Immunol. 23, 2799–2806 (1993).
17. Campanero, M. R. et al. ICAM-3 interacts with LFA-1 and regulates the LFA-1/ICAM-1 cell adhesion pathway. J. Cell Biol. 123, 1007–1016 (1993).
18. Juan, M. et al. CD50 (intercellular adhesion molecule 3) stimulation induces calcium mobilization and tyrosine phosphorylation through p59(fyn) and p56(lck) in Jurkat T cell line. J. Exp. Med. 179, 1747–1756 (1994).
19. Bleijs, D. A., de-Waal-Malefyt, R., Figdor, C. G. & van-Kooyk, Y. Co-stimulation of T cells results in distinct IL-10 and TNF-α cytokine profiles dependent on binding to ICAM-1, ICAM-2 or ICAM-3. Eur. J. Immunol. 29, 2248–2258 (1999).
20. van-der-Vieren, M. et al. A novel leukointegrin, αdβ2, binds preferentially to ICAM-3. Immunity 3, 683–690 (1995).
21. Geijtenbeek, T. B. et al. Identification of DC-SIGN, a novel dendritic cell-specific ICAM-3 receptor that supports immune responses. Cell 100, 575–585 (2000).
22. Niedergang, F., Dautry-Varsat, A. & Alcover, A. Peptide antigen or superantigen-induced down regulation of TCR involves both stimulated and unstimulated receptors. J. Immunol. 159, 1703–1710 (1997).
23. del-Pozo, M. A., Sánchez-Mateos, P., Nieto, M. & Sánchez-Madrid, F. Chemokines regulate cellular polarization and adhesion receptor redistribution during lymphocyte interaction with endothelium and extracellular matrix. Involvement of cAMP signaling pathway. J. Cell Biol. 131, 495–508 (1995).
24. Alonso-Lebrero, J. L. et al. Polarization and interaction of adhesion molecules P-selectin glycoprotein ligand 1 and intracellular adhesion molecule 3 with moesin and ezrin in myeloid cells. Blood 95, 2413–2419 (2000).
25. Negulescu, P. A., Krasieva, T. B., Khan, A., Kerschbaum, H. H. & Cahalan, M. D. Polarity of T cell shape,

motility and sensitivity to antigen. *Immunity* **4**, 421–430 (1996).

26. Lowin-Kropf, B., Shapiro, V. S. & Weiss, A. Cytoskeletal polarization of T cells is regulated by an inmunore-ceptor tyrosine-based activation motif-dependent mechanism. *J. Cell Biol.* **140**, 861–871 (1998).

27. van-Kooyk, Y. & Figdor, C. G. Avidity regulation of integrins: the driving force in leukocyte adhesion. *Curr. Opin. Cell Biol.* **12**, 542–547 (2000).

28. Dustin, M. L. & Springer, T. A. T cell receptor cross-linking transiently stimulates adhesiveness through LFA-1. *Nature* **341**, 619–624 (1989).

29. van-Kooyk, Y. *et al.* Enhancement of LFA-1 mediated cell adhesion by triggering through CD2 or CD3 on T lymphocytes. *Nature* **342**, 811–813 (1989).

30. Janes, P. W., Ley, S. C. & Magee, A. I. Aggregation of lipid rafts accompanies signaling *via* the T cell anti-gen receptor. *J. Cell Biol.* **147**, 447–461 (1999).

31. Langlet, C., Bernard, A. M., Drevot, P. & He, H. T. Membrane rafts and signaling by the multichain immune recognition receptors. *Curr. Opin. Immunol.* **12**, 250–255 (2000).

32. Davis, S. J. & van-der-Merwe, P. A. Structure and ligand interactions of CD2: implications for T-cell function. *Immunol. Today* **17**, 177–187 (1996).

33. Millan, J., Montoya, M. C., Sancho, D., Sánchez-Madrid, F. & Alonso, M. A. Lipid rafts mediate biosyn-thetic transport to the T lymphocyte uropod subdomain and are necessary for uropod integrity and function. *Blood* (2002, in the press).

34. Zhang, W., Trible, R. P. & Samelson, L. E. LAT palmitoylation: its essential role in membrane microdomain targeting and tyrosine phosphorylation during T cell activation. *Immunity* **9**, 239–246 (1998).

35. Zhang, W., Irvin, B. J., Trible, R. P., Abraham, R. T. & Samelson, L. E. Functional analysis of LAT in TCR-mediated signaling pathways using a LAT-deficient Jurkat cell line. *Int. Immunol.* **11**, 943–950 (1999).

36. Lin, J., Weiss, A. & Finco, T. S. Localization of LAT in glycolipid-enriched microdomains is required for T cell activation. *J. Biol. Chem.* **274**, 28861–28864 (1999).

37. Bosseult, R. *et al.* Association of the adaptor molecule LAT with CD4 and CD8 coreceptors identifies a new coreceptor function in T cell receptor signal transduction. *J. Exp. Med.* **190**, 1517–1525 (1999).

38. Krummel, M. F., Sjaastad, M. D., Wülfing, C. & Davis, M. M. Differential clustering of CD4 and CD3

39. Millan, J., Qaidi, M. & Alonso, M. A. Segregation of co-stimulatory components into specific T cell sur-face lipid rafts. *Eur. J. Immunol.* **31**, 467–473 (2001).

40. Sperling, A. I. *et al.* TCR signaling induces selective exclusion of CD43 from the T cell-antigen-pre-senting cell contact site. *J. Immunol.* **161**, 6459–6462 (1998).

41. Serrador, J. *et al.* Moesin interacts with the cytoplasmic region of ICAM-3 and is redistributed to the uropod of T lymphocytes during cell polarization. *J. Cell Biol.* **138**, 1409–1423 (1997).

42. del-Pozo, M. A., Arroyo, A. G., Campanero, M. R. & Sánchez-Madrid, F. Epitope mapping of ICAM-3 (CD50). *Leukocyte Typing* V, 1568–1571 (1995).

43. Hauss, P., Selz, F., Cavazzana-Calvo, M. & Ficher, A. Characteristics of antigen-independent and antigen-dependent interaction of dendritic cells with CD4+ T cells. *Eur. J. Immunol.* **25**, 2285–2294 (1995).

44. Starling, G. C. *et al.* Intercellular adhesion molecule-3 is the predominant co-stimulatory ligand for leukocyte function antigen-1 on human blood dendritic cells. *Eur. J. Immunol.* **25**, 2528–2532 (1995).

45. Griffiths, C., Railan, D., Gallatin, W. M. & Cooper, K. D. The ICAM-3/LFA-1 interaction is critical for epi-dermal Langerhans cell alloantigen presentation to CD4+ T cells. *Br. J. Dermatol.* **133**, 823–829 (1995).

46. Hernandez-Caselles, T., Martinez-Esparza, M., Lazarovits, A. I. & Aparicio, P. Specific regulation of VLA-4 and α4β7 integrin expression on human activated T lymphocytes. *J. Immunol.* **156**, 3668–3677 (1996).

47. Romani, N. *et al.* Proliferating dendritic cell progenitors in human blood. *J. Exp. Med.* **180**, 83–93 (1994).

48. Campanero, M. R., Sánchez-Mateos, P., del-Pozo, M. A. & Sánchez-Madrid, F. ICAM-3 regulates lympho-cyte morphology and integrin-mediated T cell interaction with endothelial cell and extracellular matrix ligands. *J. Cell Biol.* **127**, 867–878 (1994).

49. Cerdan, C. *et al.* Prolonged IL-2 receptor α/CD25 expression after T cell activation *via* the adhesion molecules CD2 and CD28. Demonstration of combined transcriptional and post-transcriptional reg-ulation. *J. Immunol.* **149**, 2255–2261 (1992).

50. Lara-Pezzi, E., Armesilla, A. L., Majano, P. L., Redondo, J. M. & Lopez-Cabrera, M. The hepatitis B virus HBx protein activates nuclear factor of activated T cells (NFAT) by a cyclosporin A-sensitive path-way. *EMBO J.* **17**, 7066–7077 (1998).

during T cell recognition. *Science* **289**, 1349–1352 (2000).